Published in final edited form as:

FASEB J. 2020 January ; 34(1): 1591–1601. doi:10.1096/fj.201902366R.

Phactr1 regulates Slack (KCNT1) channels via protein phosphatase 1 (PP1)

Syed Rydwan Ali[1], **Taylor Joseph Malone**[1], **Yalan Zhang**[1], **Magdalena Prechova**[3,4], **Leonard Konrad Kaczmarek**[1,2,*]

[1]Department of Pharmacology, Yale School of Medicine, New Haven, CT, USA

[2]Department of Cellular and Molecular Physiology, Yale School of Medicine, New Haven, CT, USA

[3]Signalling and Transcription Group, The Francis Crick Institute, London, UK.

[4]Laboratory of Integrative Biology, Institute of Molecular Genetics of the Czech Academy of Sciences, Prague, CZ

Abstract

The *Slack* (*KCNT1*) gene encodes sodium-activated potassium channels that are abundantly expressed in the central nervous system. Human mutations alter the function of Slack channels, resulting in epilepsy and intellectual disability. Most of the disease-causing mutations are located in the extended cytoplasmic C-terminus of Slack channels and result in increased Slack current. Previous experiments have shown that the C-terminus of Slack channels binds a number of cytoplasmic signaling proteins. One of these is Phactr1, an actin-binding protein that recruits protein phosphatase 1 (PP1) to certain phosphoprotein substrates. Using co-immunoprecipitation, we found that Phactr1 is required to link the channels to actin. Using patch clamp recordings, we found that co-expression of Phactr1 with wild type Slack channels reduces current amplitude but has no effect on Slack channels in which a conserved PKC phosphorylation site (S407) that regulates current amplitude has been mutated. Furthermore, a Phactr1 mutant that disrupts the binding of PP1 but not that of actin fails to alter Slack currents. Our data suggest that Phactr1 regulates Slack by linking PP1 to the channel. Targeting Slack-Phactr1 interactions may therefore be helpful in developing novel therapies for brain disorders associated with the malfunction of Slack channels.

INTRODUCTION

Slack potassium channels ($K_{Na}1.1$, Slo2.2, KCNT1) are activated by intracellular Na^+ and are abundantly expressed in the nervous system (1–7). Under physiological conditions, Slack

*To whom correspondence should be addressed: Leonard K. Kaczmarek, Professor of Pharmacology and Cellular and Molecular Physiology, Department of Pharmacology, Sterling Hall of Medicine, 333 Cedar Street, New Haven, Connecticut 06520-8066, Telephone: 203 785-4500, Fax: 203 785-5494, leonard.kaczmarek@yale.edu.

CONTRIBUTIONS

S.R.A. and L.K.K. conceived and designed all biophysical and neurobiology experiments. S.R.A, T.J.M. and L.K.K. wrote the manuscript. S.R.A. performed co-immunoprecipitation, immunocytochemistry. S.R.A. and Y.Z. performed patch-clamp experiments and isolated primary cortical neurons. M.P. generated and characterized the Phactr1^{humdy} mutant.

CONFLICT OF INTEREST

The authors declare no competing financial interest.

channels regulate the rate of neuronal bursting and control the accuracy of action potential timing (8–10). Human mutations alter the function of Slack channels, resulting in at least two distinct childhood epilepsies that are associated with very severe intellectual impairment (1, 5). These conditions are malignant migrating focal seizures of infancy (MMFSI, also termed EIMFS, Epilepsy of Infancy with Migrating Focal Seizures) (11, 12) and autosomal dominant frontal lobe epilepsy (ADNLFE) (6, 13). Other conditions reported for Slack mutations include leukodystrophy multifocal epilepsy(14), early onset epilepsy and encephalopathy (EOEE) (15), nocturnal frontal lobe epilepsy (NFLE) (13), leukoencephalopathy (16), Ohtahara syndrome (17) and Brugada syndrome with epilepsy (18). Most of the disease-causing mutations are located in the extended cytoplasmic C-terminus of Slack and result in increased Slack current (6, 7, 10, 19). This increase in Slack current, directly or indirectly, results in the over-excitation of the excitatory cortical neurons (10). However, the severe intellectual impairment is unlikely to be caused simply by the occurrence of the seizures, because mutations in other proteins can produce very similar seizure patterns with no resultant deficit in intellectual function (5, 13). This raises the possibility that the interactions of the Slack C-terminal domain with cytoplasmic signaling molecules have functions that go beyond the control of channel gating. The disruption of these “non-conducting” functions (20, 21) may severely disrupt neuronal function, leading to intellectual disability.

The C-terminus of Slack channels interacts with a variety of cellular signaling pathways, including fragile X mental retardation protein (FMRP) (1–3, 5, 22–24), cytoplasmic FMRP interacting protein (CYFIP1) (4) and Phosphatase and Actin Regulator 1 (Phactr1) (4). Dysregulation of these proteins is associated with Fragile X syndrome (FXS) (5, 24), schizophrenia (22, 25), amyotrophic lateral sclerosis (ALS) (26), epilepsy (22), and intellectual disability (1, 5, 24). Phactr1 is highly expressed in neurons of the cerebral cortex, where it plays a role in controlling synaptic activity and synapse morphology through regulation of protein phosphatase 1 (PP1) and actin binding (27). Phactr1 has also been implicated in the molecular mechanisms of migraine (28), infantile Spasm (West Syndrome) (29) and intellectual disability (30). Recently, it has been demonstrated that expression of Phactr1 mRNA was completely lost after traumatic brain injury (TBI) (31).

Although Phactr1 has been shown to dissociate from Slack channels following their activation or phosphorylation, the functional consequences of the Slack-Phactr1 interaction are not known (4). Recent data indicate that the Phactr1/PP1 complex is a PP1 holoenzyme (32). Phosphorylation of Slack at a serine residue (S407) in the cytoplasmic C-terminal domain by PKC increases Slack currents (11). We now show that Phactr1 links both PP1 and actin to the Slack channel complex and reduces Slack current amplitude in channels that contain the S407 site. Mutation of this site to an alanine, however, renders the channels insensitive to Phactr1 under basal conditions. Moreover, we show that wild type Slack channels are insensitive to a Phactr1 mutant that does not bind PP1 (33, 34). Our data indicate that Phactr1 is a key regulator of Slack current amplitude.

EXPERIMENTAL METHODS

Creation of mammalian expression vectors

Slack-B-GFP (rat) and Slack^{S407A} were engineered and characterized as previously described (11, 35). GFP-Phactr1 (mouse) was a gift from Maria K. Vartiainen (University of Helsinki, Finland). To generate plasmid coding Phactr1^{humdy}, site-directed mutagenesis was performed using the following set of primers:

Forward: GCCCAAGACTATGACCCAAGGGCAGACAAGCCA;

Reverse: TGGCTTGTCTGCCCTTGGGTCATAGTCTTGGGC.

All constructs were verified by DNA sequencing from Yale Keck facility.

Cell culture and transfection

HEK293T were maintained in growth medium composed of high-glucose DMEM (Invitrogen, Waltham, MA) supplemented with 10% fetal bovine serum (Sigma, St. Louis, MO), 1% penicillin/streptomycin (Life Technologies, Carlsbad, CA), 1% Na-pyruvate (Life Technologies, Carlsbad, CA) incubated at 37°C with 5% CO_2. Cells were transfected according to manufacturer's instructions at 90–100% confluency with equal amount of plasmid pairs using Lipofectamine 2000 (Invitrogen, Waltham, MA).

Co-immunoprecipitation

HEK293T cells were transiently transfected with the respective plasmids (5 μg per plasmid) in 25 cm^2 flask. The following day, cells were washed twice with PBS and lysed in Pierce IP lysis buffer (Thermo Scientific, Rockford, IL) supplemented with protease inhibitor cocktail (cOmplete Mini, EDTA-free, Roche, Indianapolis, IN). Cell extracts were collected and sonicated for 20 s and centrifuged at 4°C, at 13,000 × g for 15 min. Supernatants were collected and mixed with anti-chicken IgY (AvesLabs, Tigard, OR) incubated overnight at 4°C with agitation. Samples were then mixed with 100 μl of Anti-IgY PrecipHen beads (AvesLabs, Tigard, OR) and allowed to incubate for 2 hours. After washing five times with lysis buffer, 50 μl of 2× sample buffer (Bio-Rad, Hercules, CA) containing 5% beta mercaptoethanol was added. Lysates were then incubated for 30 min at room temperature and resolved on 4–15% polyacrylamide gradient gels (Bio-Rad, Hercules, CA). Resolved proteins were transferred to nitrocellulose membranes (Bio-Rad, Hercules, CA) for 2 h at 4°C and blocked in tris-buffered saline (TBS) with 10% Blokhen II™ (AvesLabs, Tigard, OR) and 0.1% Tween-20. The primary antibody concentrations were as follows: anti-Slack-B 1:5000 (AvesLabs, Tigard, OR), anti-Phactr1 1:1000 (Sigma-Millipore, Burlington, MA), anti-actin 1:1000 (Sigma-Millipore, Burlington, MA), and PP1 1:1000 (SantaCruz, Dallas, TX). The secondary antibody concentrations were as follows: anti-chicken 1:20000 (AvesLabs, Tigard, OR), anti-mouse 1:1000 (Invitrogen, Carlsbad, CA), and anti-rabbit 1:1000 (Invitrogen, Carlsbad, CA). Premium Autoradiography Film (Holliston, MA) was used to detect protein bands upon addition of chemiluminescence substrate (SuperSignal West Femto Maximum Sensitivity substrate, Rockford, IL). Protein bands were analyzed with ImageJ software.

Animals

Rodents were handled in accordance with protocols approved by the Yale University Institutional Animal Care Committee. Mice were housed on a 12/12 light/dark cycle with access to food and water ad libitum. Experiments were performed with *BL6/SC12* for Slack wild-type (WT) mice. Genotyping was performed by ear clip biopsy-derived genomic DNA using established polymerase chain reaction protocol with primers amplifying WT (277 bp) alleles.

Primary neuronal culture

Primary cortical neurons were prepared from E18 mice as described previously with modifications specific for this study (36). After isolation of cortex from prenatal brains, neurons were dissociated and seeded (0.2×10^6cells/6 well-plate) onto plates containing neurobasal medium (Thermo Scientific, Rockford, IL) with 5% FBS. After 2 h incubation, media was replaced and cells were maintained in neurobasal medium supplemented with B-27 (Life Technologies, Carlsbad, CA), L-glutamine and antibiotics (Invitrogen GIBCO Life Technologies, Carlsbad, CA, USA). Neurons were grown at 37 °C in 5% CO_2 and 20% O_2 in a humidified incubator.

Immunocytochemistry and image acquisition

Detailed methods for the immunocytochemistry can be found in previous studies (37). After removing the culture medium from the 6-well plate, cells were washed, fixed with 4% fresh Paraformaldehyde Fixing Solution (PFA), and permeabilized with 0.3% Triton®-X. Cells were then blocked with 5% goat serum for 1 h followed by overnight incubation of anti-Slack (1:50 dilution, Abcam, Cambridge, MA), and anti-Phactr1 (1:50 dilution, Sigma, St. Louis, MO). Cells were washed and incubated with Alexa-fluor 488 mouse-antibody or Alexa-546 rabbit-antibody (1:1000 dilution, Molecular Probes, Carlsbad, CA, USA) for 1 h at room temperature and mounted on glass slides with Vectashield^R mounting media (Burlingame, CA). Confocal images were acquired using a Leica SP8 confocal microscope with a 63x magnification. Multitrack acquisition was performed with excitation lines at 488 nm for Alexa 488, and 556 nm for Alexa 546. Z-series stack confocal images were taken at fixed intervals; frame size was either 1024 × 1024 or 512 × 512 pixels. All confocal images were processed using ImageJ US NIH (http://imagej.nih.gov/ij).

Whole-cell recording

Cells expressing green fluorescent protein (GFP) or GFP-Phactr1 were recorded 24–48 h after transfection. Electrodes had a resistance of 3–6 MΩ. The bath (extracellular) solution consisted of 140 mM NaCl, 1.0 mM $CaCl_2$, 3 mM KCl, 29 mM glucose and 25 mM HEPES (pH 7.4) and the pipette (intracellular) solution contained 32.5 mM KCl, 97.5 mM potassium gluconate, 5 mM EGTA and 10 mM HEPES (pH 7.2) (38). Macroscopic currents were recorded with an EPC7 amplifier (Molecular Devices, Union City, CA) using the whole-cell configuration of the patch-clamp technique. HEK293T cells were clamped at −80 mV and then voltage steps of 20 mV ranging from −100 to 80 mV were applied for a duration of 300 ms. Capacitance measurements were also collected and used to compute current density.

Recordings were carried out at room temperature (20–22 °C) after incubation of cells for 30 min with either with 0.2% DMSO or 200 nM TPA in the extracellular solution.

Statistical analysis

Statistical values were calculated as mean and standard error of the mean (mean ± SEM), unless otherwise specified. The statistical significance (*$p<0.05$) of different groups was determined by unpaired t-test, one-way ANOVA with *post-hoc* Dunn's method or Kruskal-Wallis one-way ANOVA on ranks with *post-hoc* Dunn's method using Graph Prism^{R} (La Jolla, CA) software.

RESULTS

Slack-Phactr1 complex interacts with PP1 and actin

It has been demonstrated previously that Slack channels directly interact with Phactr1 (4). Using primary cultures of cortical neurons, we first examined the localization of both proteins by immunocytochemistry (Fig.1 A–B). By light-level immunomicroscopy, co-localization was found both by inspection of line scans across individual cells, as well as by quantification of relative brightness of the fluorescent signal representing the two proteins in individual pixels, (Fig.1B, Pearson's R value 0.92, $p<0.0001$) (39).

Because Phactr1 is a PP1- and actin-binding protein, we tested whether Phactr1 links Slack channels to these two proteins. We transiently transfected HEK293T cells either with Slack alone or with both Slack and Phactr1 (tagged with GFP). We then immunoprecipitated the Slack channels and carried out immunoblotting for Phactr1, actin and PP1 (Fig.1 C–D). Upon Slack precipitation, we observed a small amount of endogenous Phactr1 both in the Slack alone as well as in Slack and Phactr1 transfected cells. When cells expressed only Slack, little or no actin could be detected in the immunoprecipitate. With cells that overexpressed both Slack and Phactr1, however, the levels of actin associated with the channel complex were increased at least one hundred-fold (by 11,697 ± 6273 %, n=4; paired ratio t-test, $p=0.0089$). In contrast, PP1 could readily be detected in Slack immunoprecipitates even in the absence of overexpressed Phactr1 (Fig.1 C–F). The levels of PP1 associated with the Slack-Phactr1 complex were, however, also increased compared to those for Slack alone (by 48 ± 11%, n=4, paired ratio t-test, $p=0.0119$). These results indicate that the association of actin with the channel absolutely requires Phactr1, while Phactr1 may target PP1 to select sites on the C-terminus of the channel but that some PP1 also binds the channel independently.

Slack currents are suppressed by overexpression of Phactr1

To investigate the functional effects of the interaction between Phactr1 and Slack channels, we carried out whole-cell patch clamp to measure macroscopic Slack currents in the presence and absence of Phactr1. HEK293T cells were transiently co-transfected with Slack-mCherry and GFP or with Slack-mCherry and GFP-Phactr1. We found that currents were significantly lower at all test potentials in cells co-expressing Phactr1 and Slack compared to those co-expressing GFP with the channel. Representative current traces with and without Phactr1 are shown in Fig. 2A. Current-voltage plots show that Phactr1 suppresses Slack

currents at all test potentials (Fig. 2B). The mean maximal current density attained during 300 ms command pulses to +80 mV (nA/pF) was reduced by over 50% in cells overexpressing Phactr1 (Fig.2C, 0.47 ± 0.11 nA/pF, n=12 for Slack vs 0.22 ± 0.06 nA/pF for Slack-Phactr1, n=12; unpaired t-test, p= 0.03).

Slack channel regulation by Phactr1 requires residue serine 407

Previous work using site-directed mutagenesis combined with patch-clamp recordings has demonstrated that the amplitude of Slack current is regulated by PKC phosphorylation of Slack residue S407, located in the linker region between the membrane-spanning domains and the cytoplasmic C-terminal RCK1 (regulator of conductance of K^+) domain (11). Application of PKC activators such as TPA (12-O-Tetradecanoylphorbol-13-acetate) to cells expressing wild type Slack channels leads to a 2–3 fold increase in current amplitude, but these activators have no effect on current amplitude in cells that express channels in which this serine has been mutated to an alanine (4, 11). Moreover, the stimulation of Slack channels by TPA has been shown to dissociate Phactr1 from the channel complex (4).

Because Phactr1 is a phosphatase-binding protein, we tested whether its effects on Slack current amplitude could be mediated by phosphorylation at the S407 site. HEK293T cells were transiently transfected with Slack-mCherry and GFP or with Slack-mCherry and GFP-Phactr1 and treated with TPA (200 nM) or the carrier medium DMSO (0.2%) for at least 30 minutes before recordings were performed (Fig.3 A–C). In agreement with previous studies, stimulation of Slack channels with TPA in the absence of overexpressed Phactr1 increased current amplitude almost three-fold (0.4316 ± .06 nA/pF, n = 14 for DMSO vs. 1.17 ± 0.21 nA/pF, n = 10 for TPA, Mann-Whitney test, p = 0.01; Fig. 3 A–C).

TPA also increased current amplitude in cells co-expressing Slack with Phactr1, but only restored current levels to those observed in the absence of Phactr1 (0.43 ± .07 nA/pF, n = 14 for GFP with DMSO vs. 0.18 ± 0.05 nA/pF, n = 16 for GFP-Phactr1 with DMSO vs. 0.45 ± 0.08 nA/pF for GFP-Phactr1 with TPA, n = 9, ANOVA, post hoc Tukey's multiple comparisons test, P =0.01; Fig.3 A–C). These findings indicate that Phactr1 reduces the efficacy of TPA to increase current amplitude, consistent with the hypothesis that Phactr1 and PKC act antagonistically.

We further explored the interaction of Phactr1 with Slack channels by investigating the actions of Phactr1 on channels in which this serine was mutated to an alanine, eliminating the ability of PKC to enhance current amplitude (11). HEK293T cells were transiently transfected with $Slack^{S407A}$-IRES and GFP or with $Slack^{S407A}$-IRES and GFP-Phactr1. These cells were then treated with TPA (200 nM) or control solution (DMSO, 0.2%) (Fig.4 A–C). Consistent with previous studies (11) treatment with TPA had no effect on the amplitude of S407A Slack currents (0.12 ± .02 nA/pF, n = 11 for DMSO vs. 0.09 ± 0.01 nA/pF, n = 5 for TPA, One-way ANOVA (Kruskal-Wallis) test, p = 0.9; Fig.4 A–C). Moreover, co-expression of Phactr1 with S407A Slack channels had no effect on current amplitude (0.12 ± .02 nA/pF, n = 11 for $Slack^{S407A}$ vs. 0.09 ± 0.01 nA/pF, n = 11 for $Slack^{407A}$ + Phactr1, One-way ANOVA (Kruskal-Wallis), p = 0.9; Fig.4 A–C). When TPA was applied to cells co-expressing S407A Slack with Phactr1, we observed a significant decrease in current amplitude, rather than an increase as occurs for wild type channels (Fig.4

A–C; 0.12 ± .02 nA/pF, n = 11 for Slack+Phactr1 in DMSO vs. 0.03 ± 0.01 nA/pF, n = 8 for Slack^{S407A}+Phactr1 with 200 nM TPA, One-way ANOVA (Kruskal-Wallis), p = 0.018). This suggests that, in the absence of the S407 regulatory phospho-site, TPA triggers other secondary mechanisms that suppress rather than activate Slack currents.

Recruitment of PP1 by Phactr1 suppresses Slack current

It has been shown previously that a mutation in Phactr4 that converts an arginine to proline in the conserved C-terminal PP1-binding domain (R650P), also termed the Phactr4^{humdy} mutation, abolishes the interaction of Phactr4 with PP1 but does not affect its binding to actin (34, 40). We used a construct with the corresponding mutation in Phactr1 (Phactr1^{humdy}/R536R) to test whether the ability of Phactr1 to suppress Slack currents required PP1 binding. Whole-cell patch clamp currents were recorded in HEK293T cells that were transiently co-transfected with Slack-mCherry and GFP or with Slack-mCherry and Phactr1^{humdy}. Representative current traces, current-voltage relationships, and bar graphs for maximal current density show that Phactr1^{humdy} does not suppress Slack current (Fig.5 A–C). There was no significant difference in current density between Slack channels alone vs Slack-Phactr1^{humdy} (0.25±0.04 nA/pF, n=6 for Slack vs 0.30±0.057 nA/pF for Slack-Phactr1, n=6; unpaired t-test, p= 0.1). These results indicate that recruitment of PP1 by Phactr1 is essential for suppressing Slack current.

DISCUSSION

Mutations in the human *Slack* gene result in several conditions in which early onset epilepsy is linked to severe intellectual disability (5). These mutations produce between two- and fifteen-fold increases in Slack current in heterologous expression systems (5–7, 11, 17, 41) as well as in human IPS cell-derived neurons (10). The amplitude of Slack currents has also been shown to be regulated by direct phosphorylation of a serine residue, S407, in the cytoplasmic C-terminal domain. Phosphorylation of this site by protein kinase C leads to rapid increases in Slack current amplitude (11, 42). For some of the disease-causing mutations, it has been shown that they behave as channels that are constitutively phosphorylated at this site (11).

One of the mechanisms that has been proposed to explain how mutations lead to neuronal dysfunction is an alteration in the interactions of Slack channels with its cytoplasmic binding partners (5) (43). In addition to Phactr1, a number of other proteins have been identified as Slack-interacting binding partners of Slack channels including FMRP, PSD95, CYFIP1 and TMEM16C (4, 44, 45). Thus far, however, only for Phactr1 is there direct evidence that these interactions are altered in disease-causing Slack mutant channels (4). Phactr1 is an ancillary protein of the Slack channel which was first identified as a binding partner by yeast-two hybrid assay (4). This protein is a member of the phosphatase and actin regulator family of proteins, which are highly expressed in the central nervous system and at lower levels also in heart, lung, kidney and testis (27, 28, 46, 47). A number of disorders such as traumatic brain injury, migraine, and myocardial infarction are related to malfunction of Phactr1 (28, 46, 47). Furthermore, Phactr1 mutations have been implicated in intellectual

disability, most likely because these mutations alter the binding of PP1 and actin (27, 29, 30).

We have found that the interaction of Slack with Phactr1 regulates the amplitude of Slack currents. Phactr1 can be co-localized with the channel in primary cortical neurons (Fig.1 A–B). Co-immunoprecipitation experiments showed that the binding of Phactr1 to Slack channels recruits both actin and PP1 to the channel complex (Fig.1). While the binding of Phactr1 appears to be an absolute requirement for the association of actin with the Slack complex, significant binding of PP1 was observed without co-expression with Phactr1. Although we cannot eliminate the possibility that the binding of PP1 is mediated by lower levels of endogenous Phactr1 in the cells, it is also possible that the cytoplasmic C-terminal domain of Slack channels binds PP1 independently of Phactr1. Consistent with this notion, there are three consensus VxF motifs for PP1 binding in this region, as has been found for cytoplasmic domains of other potassium channels that interact with this phosphatase (48).

Two lines of evidence strongly suggest that the suppression of Slack currents under basal conditions by Phactr1 is dependent on its ability to recruit PP1, and involves dephosphorylation of Slack serine 407 (11) (Figure 6A). First, expression of Phactr1 had no effect on $Slack^{S407A}$ channels, which cannot be phosphorylated at this site. Second, expression of a Phactr1 mutant ($Phactr1^{humdy}$) that can bind actin but cannot bind PP1 had no effect on Slack current under basal conditions. These observations suggest that phospho-S407 might be a direct target for dephosphorylation by PP1 which is linked to Phactr1. Two other findings suggest, however, that the interaction of Phactr1 with Slack channel could be more complex than simply acting as an adaptor that targets PP1 to S407. First, the protein sequence surrounding S407 does not resemble the optimal sites for dephosphorylation by the Phactr1/PP1 complex (32). Secondly, current of $Slack^{S407A}$ channel is suppressed rather than enhanced by TPA, selectively in the presence of Phactr1. This finding suggests that, when all four Slack subunits are fully dephosphorylated at S407, the interaction of Phactr1 with the channel recruits a second, PKC-dependent, mechanism to further suppress Slack currents (Figure 6B). The nature of this process is not known but could involve the binding of actin and/or dephosphorylation of additional sites on the channel to reduce current by altering channel gating or removing channels from the plasma membrane.

We suggest that the normal suppression of Slack currents by its interaction with Phactr1 may be reduced or missing in human mutant Slack channels that produce early onset epilepsy and intellectual disability. This is consistent with three findings: i) most of disease-causing mutations are gain-of-function channel mutations that increase potassium current (6, 7, 11, 17), (but see reference 19), ii) some of these mutations have been found to act as if they are constitutively phosphorylated (11), and iii) Slack-Phactr1 interactions have been found to be abnormal in these mutations (4). Thus, the Slack-Phactr1 interaction may represent a target for developing novel therapeutics toward these devastating diseases.

ACKNOWLEDGEMENTS

The authors acknowledge the Center for Cellular and Molecular Imaging and Physiology Imaging Facility at Yale University School of Medicine. We thank Roman Fedorshchak and Richard Treisman for helpful discussions, and for suggesting the $Phactr1^{humdy}$ experiment.

FUNDING

This work is supported by NIH R01DC001919 (LKK), NIH 1R01NS102239, FRAXA (LKK), Eunice Kennedy Shriver National Institute of Child Health & Human Development of the National Institutes of Health Fellowship under Award Number F32HD093292 (SRA), and NIH Grant GM007324 (TJM).

Abbreviations:

PP1	Protein phosphatase 1
PKC	Protein kinase C
DMSO	Dimethyl sulfoxide
FMRP	fragile X mental retardation protein
CYFIP1	cytoplasmic FMRP interacting protein
PBS	Phosphate-buffered saline
PHACTR1	Phosphatase And Actin Regulator 1
FBS	fetal bovine serum
TPA	12-O-Tetradecanoylphorbol-13-acetate
FXS	Fragile X syndrome
ALS	amyotrophic lateral sclerosis

References

1. Bausch AE, Dieter R, Nann Y, Hausmann M, Meyerdierks N, Kaczmarek LK, Ruth P, and Lukowski R (2015) The sodium-activated potassium channel Slack is required for optimal cognitive flexibility in mice. Learn Mem 22, 323–335 [PubMed: 26077685]
2. Brown MR, Kronengold J, Surguchev AA, and L.K. K (2014) Mutations in FMRP prevent FMRP-Slack potassium channel interactions on the plasma membrane. . Neurosci. Abstr, (CD ROM), 12608
3. Brown MR, Kronengold J, Gazula VR, Chen Y, Strumbos JG, Sigworth FJ, Navaratnam D, and Kaczmarek LK (2010) Fragile X mental retardation protein controls gating of the sodium-activated potassium channel Slack. Nature neuroscience 13, 819–821 [PubMed: 20512134]
4. Fleming MR, Brown MR, Kronengold J, Zhang Y, Jenkins DP, Barcia G, Nabbout R, Bausch AE, Ruth P, Lukowski R, Navaratnam DS, and Kaczmarek LK (2016) Stimulation of Slack K+ Channels Alters Mass at the Plasma Membrane by Triggering Dissociation of a Phosphatase-Regulatory Complex. Cell Rep 16, 2281–2288 [PubMed: 27545877]
5. Kim GE, and Kaczmarek LK (2014) Emerging role of the KCNT1 Slack channel in intellectual disability. Front Cell Neurosci 8, 209 [PubMed: 25120433]
6. Kim GE, Kronengold J, Barcia G, Quraishi IH, Martin HC, Blair E, Taylor JC, Dulac O, Colleaux L, Nabbout R, and Kaczmarek LK (2014) Human slack potassium channel mutations increase positive cooperativity between individual channels. Cell Rep 9, 1661–1672 [PubMed: 25482562]
7. Tang QY, Zhang FF, Xu J, Wang R, Chen J, Logothetis DE, and Zhang Z (2016) Epilepsy-Related Slack Channel Mutants Lead to Channel Over-Activity by Two Different Mechanisms. Cell Rep 14, 129–139 [PubMed: 26725113]
8. Foehring RC, Schwindt PC, and Crill WE (1989) Norepinephrine selectively reduces slow Ca2+- and Na+-mediated K+ currents in cat neocortical neurons. Journal of neurophysiology 61, 245–256 [PubMed: 2918353]

9. Yang B, Desai R, and Kaczmarek LK (2007) Slack and Slick K(Na) channels regulate the accuracy of timing of auditory neurons. J Neurosci 27, 2617–2627 [PubMed: 17344399]

10. Quraishi IH, Stern S, Mangan KP, Zhang Y, Ali SR, Mercier MR, Marchetto MC, McLachlan MJ, Jones EM, Gage FH, and Kaczmarek LK (2019) An Epilepsy-Associated KCNT1 Mutation Enhances Excitability of Human iPSC-Derived Neurons by Increasing Slack KNa Currents. J Neurosci 39, 7438–7449 [PubMed: 31350261]

11. Barcia G, Fleming MR, Deligniere A, Gazula VR, Brown MR, Langouet M, Chen H, Kronengold J, Abhyankar A, Cilio R, Nitschke P, Kaminska A, Boddaert N, Casanova JL, Desguerre I, Munnich A, Dulac O, Kaczmarek LK, Colleaux L, and Nabbout R (2012) De novo gain-of-function KCNT1 channel mutations cause malignant migrating partial seizures of infancy. Nat Genet 44, 1255–1259 [PubMed: 23086397]

12. Ishii A, Shioda M, Okumura A, Kidokoro H, Sakauchi M, Shimada S, Shimizu T, Osawa M, Hirose S, and Yamamoto T (2013) A recurrent KCNT1 mutation in two sporadic cases with malignant migrating partial seizures in infancy. Gene

13. Heron SE, Smith KR, Bahlo M, Nobili L, Kahana E, Licchetta L, Oliver KL, Mazarib A, Afawi Z, Korczyn A, Plazzi G, Petrou S, Berkovic SF, Scheffer IE, and Dibbens LM (2012) Missense mutations in the sodium-gated potassium channel gene KCNT1 cause severe autosomal dominant nocturnal frontal lobe epilepsy. Nature genetics 44, 1188–1190 [PubMed: 23086396]

14. Arai-Ichinoi N, Uematsu M, Sato R, Suzuki T, Kudo H, Kikuchi A, Hino-Fukuyo N, Matsumoto M, Igarashi K, Haginoya K, and Kure S (2016) Genetic heterogeneity in 26 infants with a hypomyelinating leukodystrophy. Hum Genet 135, 89–98 [PubMed: 26597493]

15. Ohba C, Kato M, Takahashi N, Osaka H, Shiihara T, Tohyama J, Nabatame S, Azuma J, Fujii Y, Hara M, Tsurusawa R, Inoue T, Ogata R, Watanabe Y, Togashi N, Kodera H, Nakashima M, Tsurusaki Y, Miyake N, Tanaka F, Saitsu H, and Matsumoto N (2015) De novo KCNT1 mutations in early-onset epileptic encephalopathy. Epilepsia 56, e121–128 [PubMed: 26140313]

16. Vanderver A, Simons C, Schmidt JL, Pearl PL, Bloom M, Lavenstein B, Miller D, Grimmond SM, and Taft RJ (2014) Identification of a novel de novo p.Phe932Ile KCNT1 mutation in a patient with leukoencephalopathy and severe epilepsy. Pediatr Neurol 50, 112–114 [PubMed: 24120652]

17. Martin HC, Kim GE, Pagnamenta AT, Murakami Y, Carvill GL, Meyer E, Copley RR, Rimmer A, Barcia G, Fleming MR, Kronengold J, Brown MR, Hudspith KA, Broxholme J, Kanapin A, Cazier JB, Kinoshita T, Nabbout R, Consortium WGS, Bentley D, McVean G, Heavin S, Zaiwalla Z, McShane T, Mefford HC, Shears D, Stewart H, Kurian MA, Scheffer IE, Blair E, Donnelly P, Kaczmarek LK, and Taylor JC (2014) Clinical whole-genome sequencing in severe early-onset epilepsy reveals new genes and improves molecular diagnosis. Human molecular genetics 23, 3200–3211 [PubMed: 24463883]

18. Juang JM, Lu TP, Lai LC, Ho CC, Liu YB, Tsai CT, Lin LY, Yu CC, Chen WJ, Chiang FT, Yeh SF, Lai LP, Chuang EY, and Lin JL (2014) Disease-targeted sequencing of ion channel genes identifies de novo mutations in patients with non-familial Brugada syndrome. Sci Rep 4, 6733 [PubMed: 25339316]

19. Evely KM, Pryce KD, and Bhattacharjee A (2017) The Phe932Ile mutation in KCNT1 channels associated with severe epilepsy, delayed myelination and leukoencephalopathy produces a loss-of-function channel phenotype. Neuroscience 351, 65–70 [PubMed: 28366665]

20. Lee A, Fakler B, Kaczmarek LK, and Isom LL (2014) More than a pore: ion channel signaling complexes. J Neurosci 34, 15159–15169 [PubMed: 25392484]

21. Kaczmarek LK (2006) Non-conducting functions of voltage-gated ion channels. Nature Reviews Neuroscience 7, 761–771 [PubMed: 16988652]

22. Abekhoukh S, Sahin HB, Grossi M, Zongaro S, Maurin T, Madrigal I, Kazue-Sugioka D, Raas-Rothschild A, Doulazmi M, Carrera P, Stachon A, Scherer S, Nascimento MR, Trembleau A, Arroyo I, Peter S, Smith IM, Mila M, Smith AC, Giangrande A, Caille I, and Bardoni B (2017) New insights into the regulatory function of CYFIP1 in the context of WAVE- and FMRP-containing complexes. Dis Model Mech

23. Huang Y (2015) Up-regulated cytoplasmic FMRP-interacting protein 1 in intractable temporal lobe epilepsy patients and a rat model. Int J Neurosci, 1–10

24. Zhang Y, Brown MR, Hyland C, Chen Y, Kronengold J, Fleming MR, Kohn AB, Moroz LL, and Kaczmarek LK (2012) Regulation of neuronal excitability by interaction of fragile X mental

retardation protein with slack potassium channels. J Neurosci 32, 15318–15327 [PubMed: 23115170]

25. Pathania M, Davenport EC, Muir J, Sheehan DF, Lopez-Domenech G, and Kittler JT (2014) The autism and schizophrenia associated gene CYFIP1 is critical for the maintenance of dendritic complexity and the stabilization of mature spines. Transl Psychiatry 4, e374 [PubMed: 24667445]
26. Zhang Y, Ni W, Horwich AL, and Kaczmarek LK (2017) An ALS-Associated Mutant SOD1 Rapidly Suppresses KCNT1 (Slack) Na+-Activated K+ Channels in Aplysia Neurons. J Neurosci 37, 2258–2265 [PubMed: 28119399]
27. Allen PB, Greenfield AT, Svenningsson P, Haspeslagh DC, and Greengard P (2004) Phactrs 1–4: A family of protein phosphatase 1 and actin regulatory proteins. Proc Natl Acad Sci U S A 101, 7187–7192 [PubMed: 15107502]
28. Freilinger T, Anttila V, de Vries B, Malik R, Kallela M, Terwindt GM, Pozo-Rosich P, Winsvold B, Nyholt DR, van Oosterhout WP, Artto V, Todt U, Hamalainen E, Fernandez-Morales J, Louter MA, Kaunisto MA, Schoenen J, Raitakari O, Lehtimaki T, Vila-Pueyo M, Gobel H, Wichmann E, Sintas C, Uitterlinden AG, Hofman A, Rivadeneira F, Heinze A, Tronvik E, van Duijn CM, Kaprio J, Cormand B, Wessman M, Frants RR, Meitinger T, Muller-Myhsok B, Zwart JA, Farkkila M, Macaya A, Ferrari MD, Kubisch C, Palotie A, Dichgans M, van den Maagdenberg AM, and International Headache Genetics C (2012) Genome-wide association analysis identifies susceptibility loci for migraine without aura. Nat Genet 44, 777–782 [PubMed: 22683712]
29. Hamada N, Ogaya S, Nakashima M, Nishijo T, Sugawara Y, Iwamoto I, Ito H, Maki Y, Shirai K, Baba S, Maruyama K, Saitsu H, Kato M, Matsumoto N, Momiyama T, and Nagata KI (2018) De novo PHACTR1 mutations in West syndrome and their pathophysiological effects. Brain 141, 3098–3114 [PubMed: 30256902]
30. de Ligt J, Willemsen MH, van Bon BW, Kleefstra T, Yntema HG, Kroes T, Vulto-van Silfhout AT, Koolen DA, de Vries P, Gilissen C, del Rosario M, Hoischen A, Scheffer H, de Vries BB, Brunner HG, Veltman JA, and Vissers LE (2012) Diagnostic exome sequencing in persons with severe intellectual disability. N Engl J Med 367, 1921–1929 [PubMed: 23033978]
31. Kim JY, Choi SY, Moon Y, Kim HJ, Chin JH, Kim H, and Sun W (2012) Different expression patterns of Phactr family members in normal and injured mouse brain. Neuroscience 221, 37–46 [PubMed: 22766235]
32. Prechova M (2018) Functional Analysis of PP1 Regulator Phactr1 In Signalling and Transcription Group, University College Londoon, London (https://ethos.bl.uk/OrderDetails.do?uin=uk.bl.ethos.747580)
33. Wiezlak M, Diring J, Abella J, Mouilleron S, Way M, McDonald NQ, and Treisman R (2012) G-actin regulates the shuttling and PP1 binding of the RPEL protein Phactr1 to control actomyosin assembly. J Cell Sci 125, 5860–5872 [PubMed: 22976292]
34. Kim TH, Goodman J, Anderson KV, and Niswander L (2007) Phactr4 regulates neural tube and optic fissure closure by controlling PP1-, Rb-, and E2F1-regulated cell-cycle progression. Dev Cell 13, 87–102 [PubMed: 17609112]
35. Chen H, Kronengold J, Yan Y, Gazula VR, Brown MR, Ma L, Ferreira G, Yang Y, Bhattacharjee A, Sigworth FJ, Salkoff L, and Kaczmarek LK (2009) The N-terminal domain of Slack determines the formation and trafficking of Slick/Slack heteromeric sodium-activated potassium channels. J Neurosci 29, 5654–5665 [PubMed: 19403831]
36. Park HA, Licznerski P, Mnatsakanyan N, Niu Y, Sacchetti S, Wu J, Polster BM, Alavian KN, and Jonas EA (2017) Inhibition of Bcl-xL prevents pro-death actions of DeltaN-Bcl-xL at the mitochondrial inner membrane during glutamate excitotoxicity. Cell Death Differ 24, 1963–1974 [PubMed: 28777375]
37. Brewer GJ, Torricelli JR, Evege EK, and Price PJ (1993) Optimized survival of hippocampal neurons in B27-supplemented Neurobasal, a new serum-free medium combination. J Neurosci Res 35, 567–576 [PubMed: 8377226]
38. Joiner WJ, Tang MD, Wang LY, Dworetzky SI, Boissard CG, Gan L, Gribkoff VK, and Kaczmarek LK (1998) Formation of intermediate-conductance calcium-activated potassium channels by interaction of Slack and Slo subunits. Nat Neurosci 1, 462–469 [PubMed: 10196543]

39. Dunn KW, Kamocka MM, and McDonald JH (2011) A practical guide to evaluating colocalization in biological microscopy. American journal of physiology. Cell physiology 300, C723–742 [PubMed: 21209361]
40. Zhang Y, Kim TH, and Niswander L (2012) Phactr4 regulates directional migration of enteric neural crest through PP1, integrin signaling, and cofilin activity. Genes Dev 26, 69–81 [PubMed: 22215812]
41. Milligan CJ, Li M, Gazina EV, Heron SE, Nair U, Trager C, Reid CA, Venkat A, Younkin DP, Dlugos DJ, Petrovski S, Goldstein DB, Dibbens LM, Scheffer IE, Berkovic SF, and Petrou S (2014) KCNT1 gain of function in 2 epilepsy phenotypes is reversed by quinidine. Ann Neurol 75, 581–590 [PubMed: 24591078]
42. Santi CM, Ferreira G, Yang B, Gazula VR, Butler A, Wei A, Kaczmarek LK, and Salkoff L (2006) Opposite regulation of Slick and Slack K+ channels by neuromodulators. J Neurosci 26, 5059–5068 [PubMed: 16687497]
43. Lim CX, Ricos MG, Dibbens LM, and Heron SE (2016) KCNT1 mutations in seizure disorders: the phenotypic spectrum and functional effects. J Med Genet 53, 217–225 [PubMed: 26740507]
44. Kaczmarek LK (2013) Slack, Slick and Sodium-Activated Potassium Channels. ISRN Neurosci 2013
45. Huang F, Wang X, Ostertag EM, Nuwal T, Huang B, Jan YN, Basbaum AI, and Jan LY (2013) TMEM16C facilitates Na(+)-activated K+ currents in rat sensory neurons and regulates pain processing. Nat Neurosci 16, 1284–1290 [PubMed: 23872594]
46. Ito H, Mizuno M, Noguchi K, Morishita R, Iwamoto I, Hara A, and Nagata KI (2018) Expression analyses of Phactr1 (phosphatase and actin regulator 1) during mouse brain development. Neurosci Res 128, 50–57 [PubMed: 28803787]
47. Kelloniemi A, Szabo Z, Serpi R, Napankangas J, Ohukainen P, Tenhunen O, Kaikkonen L, Koivisto E, Bagyura Z, Kerkela R, Leosdottir M, Hedner T, Melander O, Ruskoaho H, and Rysa J (2015) The Early-Onset Myocardial Infarction Associated PHACTR1 Gene Regulates Skeletal and Cardiac Alpha-Actin Gene Expression. PLoS One 10, e0130502 [PubMed: 26098115]
48. Kang S, Xu M, Cooper EC, and Hoshi N (2014) Channel-anchored protein kinase CK2 and protein phosphatase 1 reciprocally regulate KCNQ2-containing M-channels via phosphorylation of calmodulin. J Biol Chem 289, 11536–11544 [PubMed: 24627475]

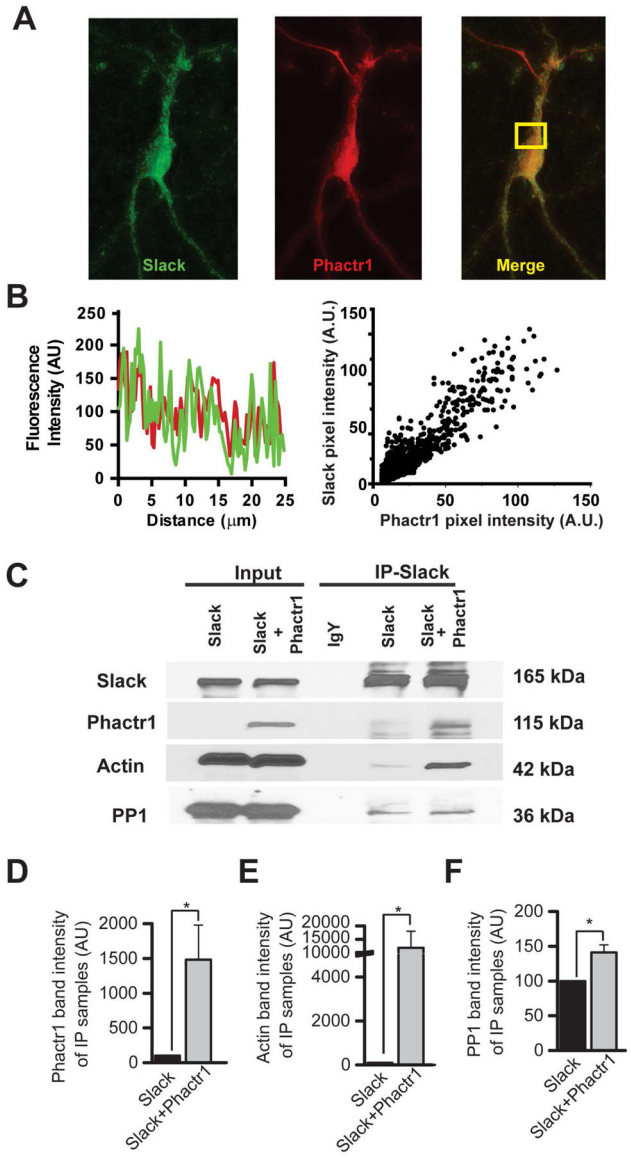

Figure 1. Actin and PP1 can be immunoprecipitated using the Slack-Phactr1 interaction as "bait".

A: Representative confocal images showing colocalization of Slack (green) and Phactr1 (red) in a primary cortical neuron. **B:** Representative example of Slack (green) and Phactr1 (red) immunofluorescence line scans in a cortical neuron (left panel) and scattergram showing the correlation of Slack and Phactr1 immunofluorescence (right panel). **C:** HEK293T cells were transiently transfected either with Slack-GFP or with Slack-GFP and the GFP-Phactr1 construct. Co-immunoprecipitation was performed using anti-Slack antibodies followed by western blotting with anti-Slack, anti-Phactr1, anti-actin or anti-PP1 antibodies. **D-F:** Densitometry analysis of Phactr1, actin, and PP1 in immunoprecipitates. Data are shown as mean ± SEM; *p < 0.05

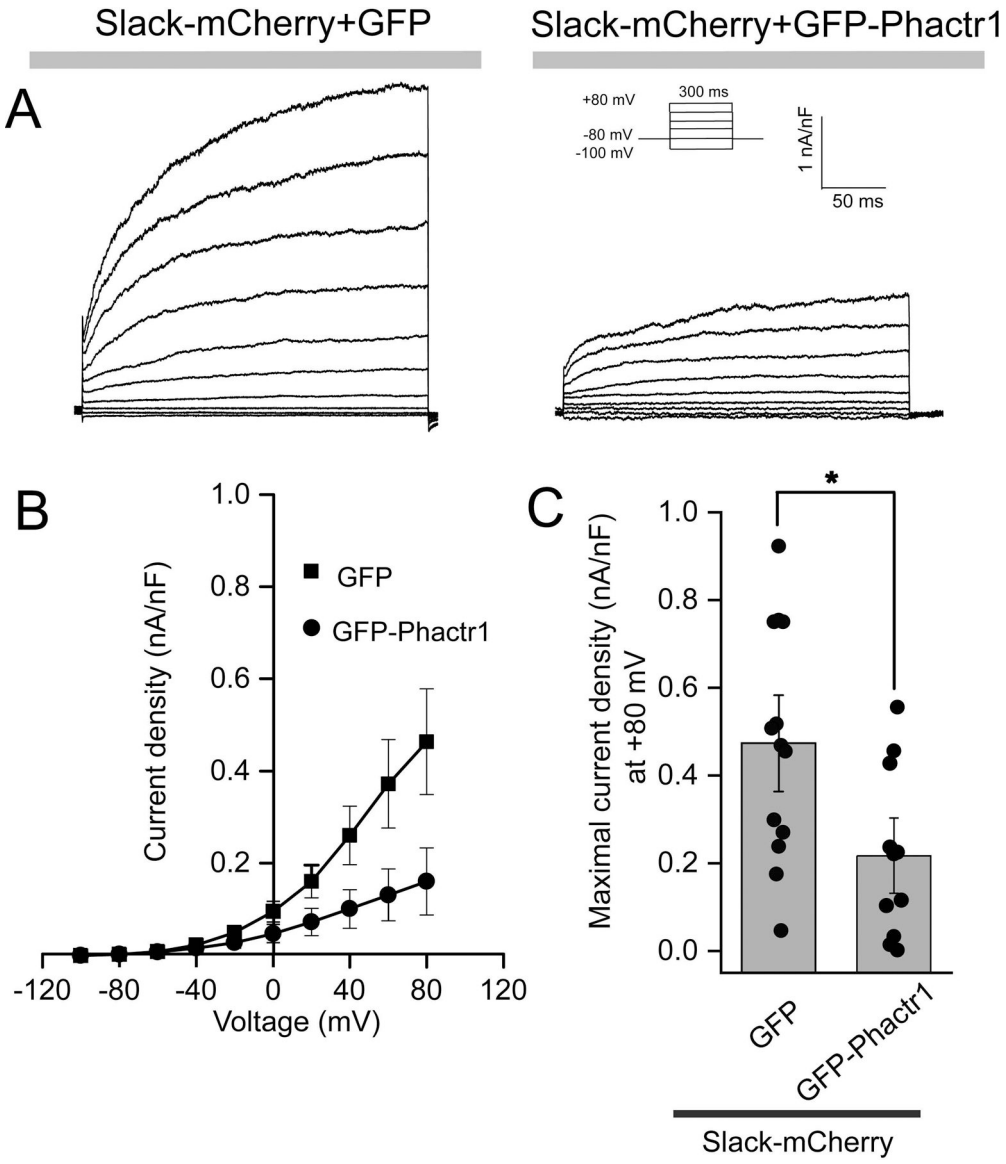

Figure 2. Phactr1 suppresses Slack current.

A: Representative traces were recorded from HEK293T cells transiently expressing Slack-mCherry with either GFP or GFP-Phactr1. **B:** Current-Voltage relationship. **C:** Bar graph summary of maximal current amplitude attained during 300 msec command pulses to +80 mV. Data are shown as mean ± SEM; *p < 0.05.

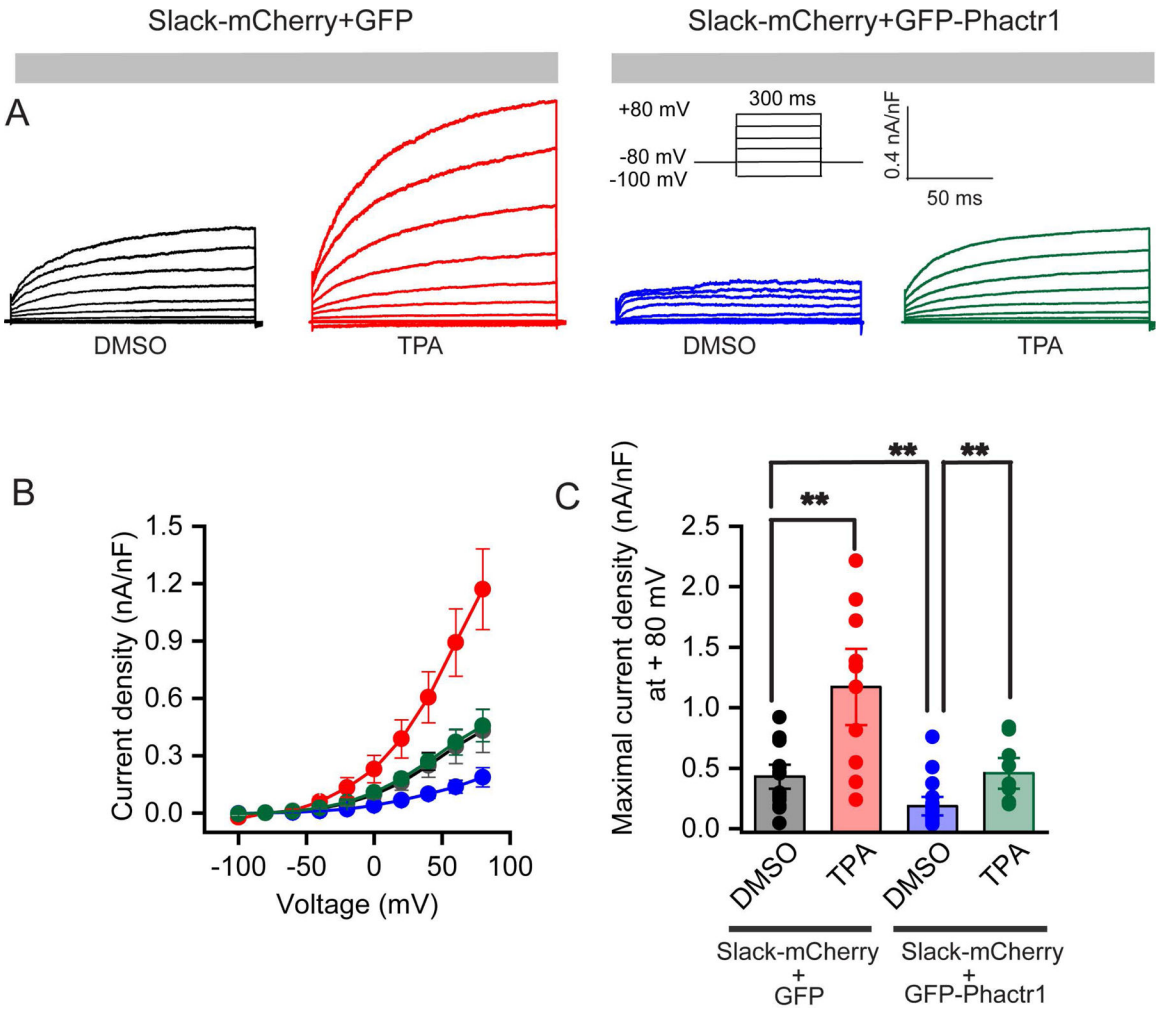

Figure 3. Stimulation of Slack by PKC enhances current.

A: Representative traces were recorded from HEK293T cells transiently expressing Slack-mCherry and GFP (DMSO, black), or Slack-mCherry and GFP (TPA, red) or Slack-mCherry and GFP-Phactr1 (DMSO, blue) or Slack-mCherry and GFP-Phactr1 (TPA, green) in response to voltage steps from −100 mV to +80 mV from a holding potential of −80 mV (protocol in inset). Cells were incubated either with 0.2% DMSO or 200 nM TPA in extracellular solution for 30 min before recordings were performed. **B:** Current-Voltage relationship of Slack current from the groups labeled in Panel A. **C:** Bar graphs representing maximal current densities measured at + 80 mV in individual cells HEK293T cells expressing the constructs described above. Data are shown as mean ± SEM; **p < 0.01.

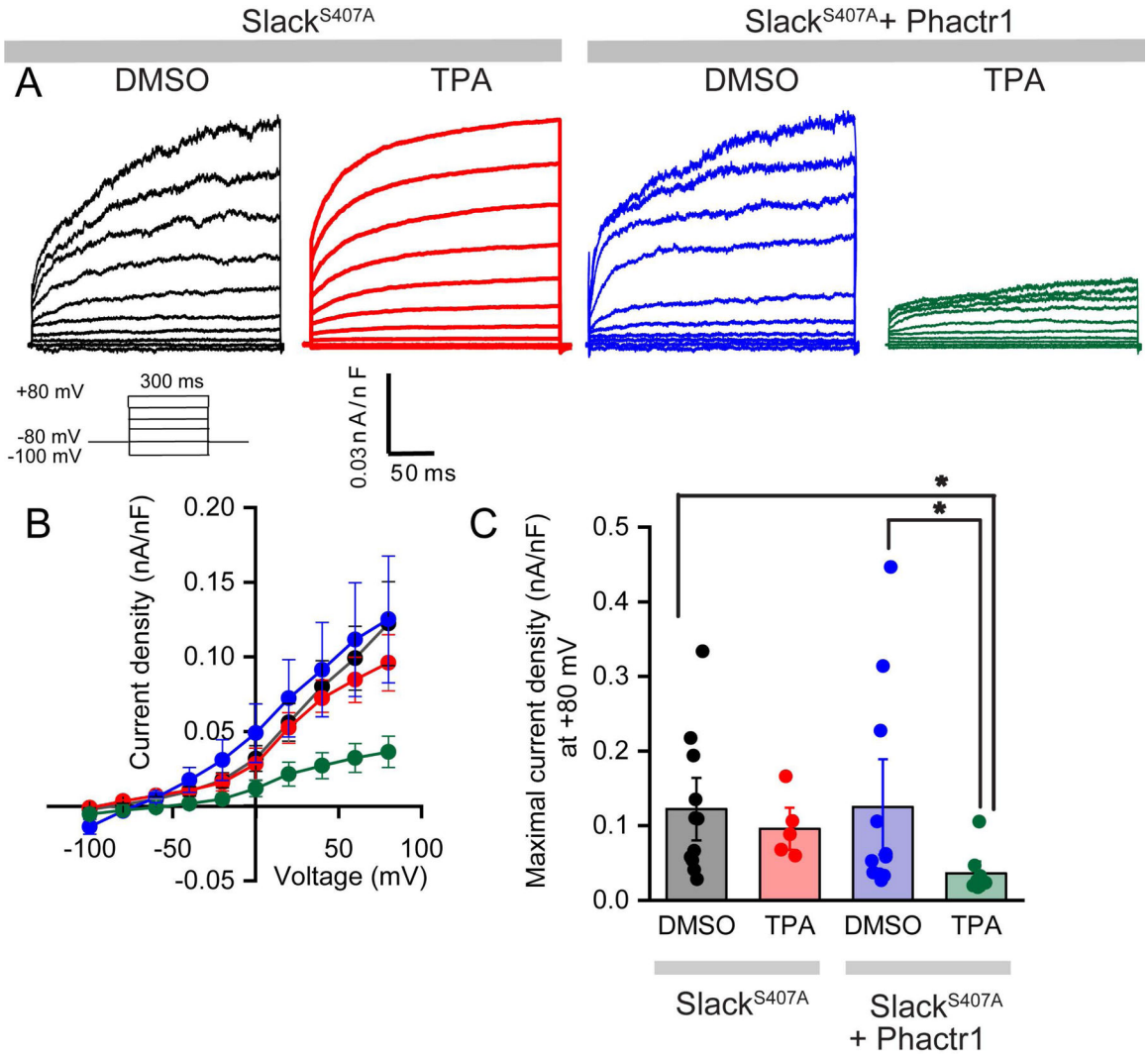

Figure 4. Phactr1 regulates Slack channels phosphorylation at the S407 site.

A: Representative traces were recorded from HEK293T cells transiently expressing Slack^{S407A}-mCherry (DMSO, black) or Slack^{S407A}-mCherry (TPA, red) or Slack^{S407A}-mCherry and Phactr1 (DMSO, blue) or Slack^{S407A}-mCherry and Phactr1 (TPA, green) in response to voltage steps from −100 mV to +80 mV from a holding potential of −80 mV. Cells were incubated either with 0.2% DMSO or 200 nM TPA in extracellular solution for 30 min before recordings were begun. **B:** Current-Voltage relationship of Slack current from groups mentioned in Panel A. **C:** Bar graphs representing maximal current densities measured at + 80 mV in individual cells HEK293T cells expressing the constructs labeled in Panel A. Data are shown as mean ± SEM; *p < 0.05.

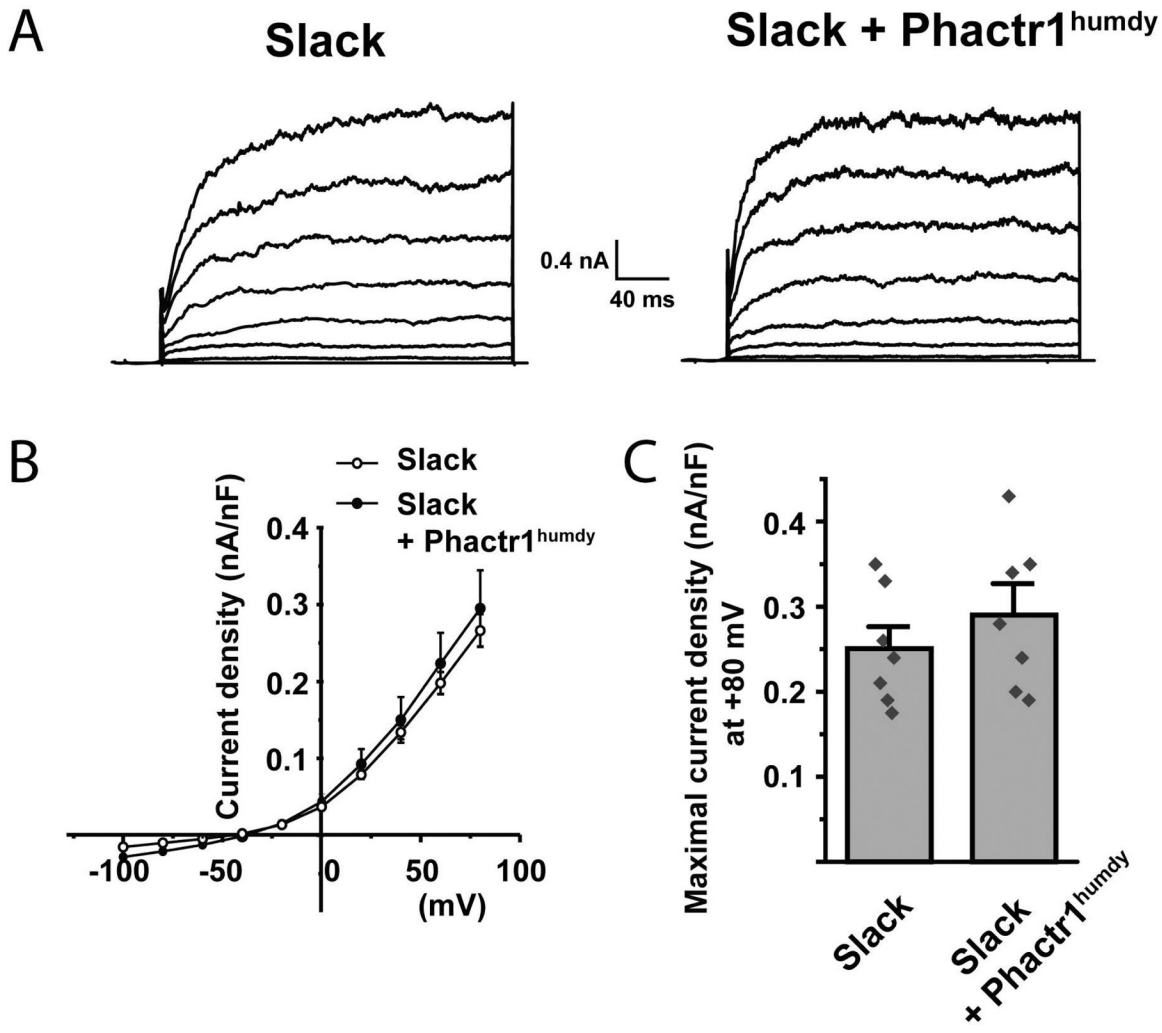

Figure 5. Phactr1^{humdy} (R536P) does not suppress Slack currents.

A: Representative traces were recorded from HEK293T cells transiently expressing Slack-mCherry or Slack-mCherry with Phactr1^{Humdy} in response to voltage steps from −100 mV to +80 mV from a holding potential of −80 mV. **B:** Current-Voltage relationship of Slack current in the two groups. **C:** Bar graphs representing maximal current densities measured during 300 msec command pulses to+ 80 mV in individual cells HEK293T cells expressing the constructs mentioned in Panel A. Data are shown as mean ± SEM.

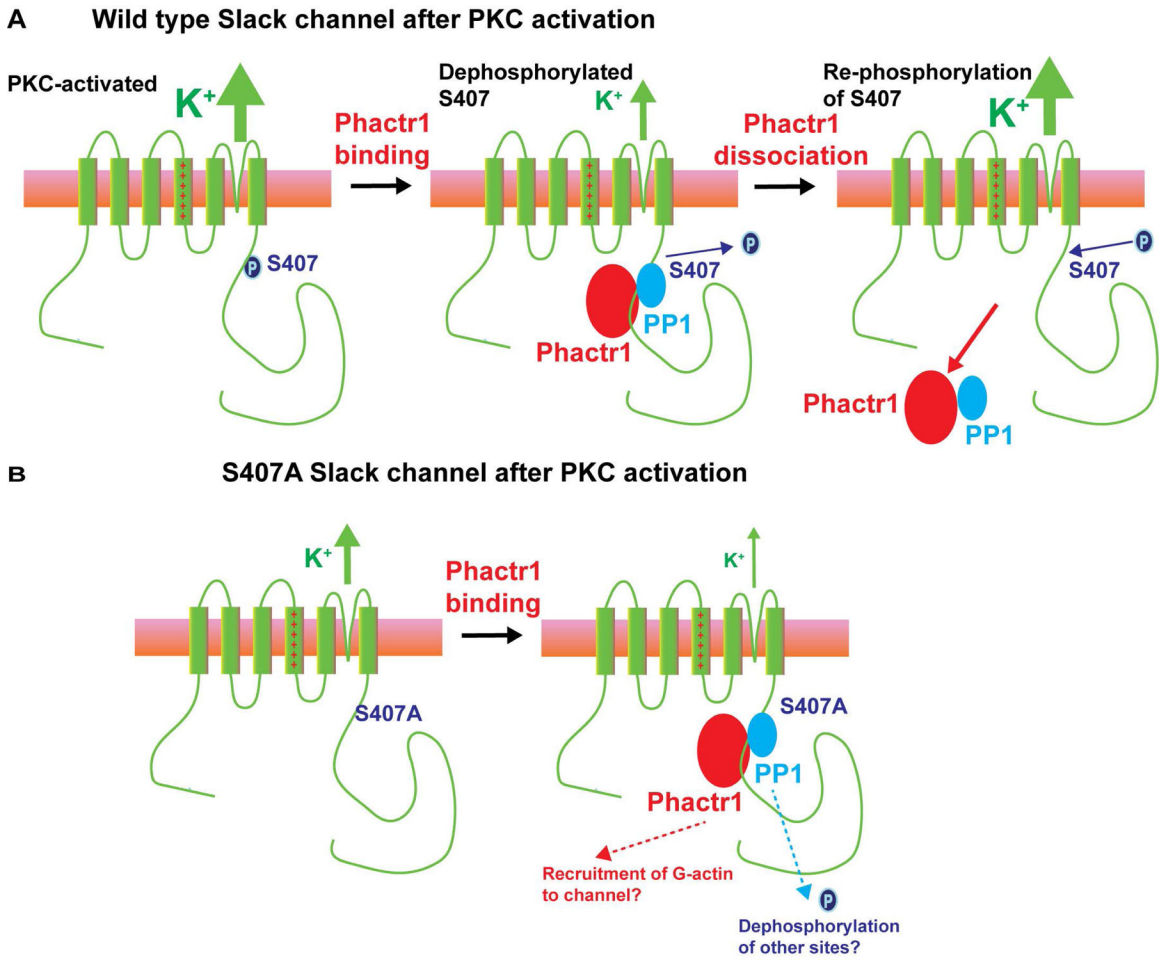

Figure 6. Potential modes of regulation of Slack channels by Phactr1.

A. In wild type Slack channels, activation of PKC causes phosphorylation of serine 407, enhancing Slack channel activity. Binding of Phactr1 recruits PP1 to the channel complex, resulting in either direct or indirect dephosphorylation of serine 407 and reversal of PKC enhancement of channel activity. Published work indicates that Phactr1 dissociates from the channel complex after phosphorylation of S407 (4). **B**. In S407A channels, which cannot be phosphorylated at this site, PKC has no effect on channel activity. In this condition, which mimics that of channels in which all four subunits are dephosphorylated at S407, recruitment of Phactr1 acts through a second independent mechanism to further suppress channel activity.